Struct Multidisc Optim (2010) 41:621–635
DOI 10.1007/s00158-009-0435-8

INDUSTRIAL APPLICATION

Multidisciplinary optimization of injection molding systems

Irene Ferreira · Olivier de Weck · Pedro Saraiva · José Cabral

Received: 11 September 2008 / Revised: 4 August 2009 / Accepted: 25 August 2009 / Published online: 6 October 2009

Abstract The design of injection molding systems for plastic parts relies heavily on experience and intuition. Recently, mold makers have been compelled to shorten lead times, reduce costs and improve process performance due to global competition. This paper presents a framework, based on a Multidisciplinary Design Optimization (MDO) methodology, which tackles the design of an injection mold by integrating the structural, feeding, ejection and heat-exchange sub-systems to achieve significant improvements. To validate it single objective optimization is presented leading to a 42% reduction in cycle time. We also perform multiple objective optimization simultaneously minimizing cycle time, wasted material and pressure drop. Sensitivity analysis shows a large impact of the sprue diameter (>1.5 normalized sensitivity) highlighting the importance of the feeding subsystem on overall quality. The results show substantial improvements resulting in reduced rework and time savings for the entire mold design process.

Keywords Injection mold design · MDO · Global design · Cycle time

I. Ferreira (✉) · O. de Weck
Engineering Systems Division (ESD),
Massachusetts Institute of Technology,
Cambridge, MA 02139, USA
e-mail: iferreira@estg.ipleiria.pt

P. Saraiva
Chemical Engineering Department, University of Coimbra,
Coimbra, Portugal

J. Cabral
Engineering Faculty, University of Porto, Porto, Portugal

Nomenclature

d_{Sprue}	Sprue diameter [m]
l_{Runner}	Runner length [m]
l_{Gate}	Gate length [m]
d_{Gate}	Gate diameter [m]
α_{Sprue}	Sprue draft angle [°]
l_{Sprue}	Sprue length [m]
P_{inj}	Injection pressure [Pa]
d_{Runner}	Runner diameter [m]
n_{Ramif}	Number of ramifications of runners
$n_{\text{downstream}}$	Number of ramification streams
n_{Gate}	Number of gates' points per part
d_{Release}	Distance of part's release [m]
α	Coefficient of diffusitivity [m^2/s]
A_{proj}	Projected area of molded part [m^2]

1 Introduction

An injection mold is a high precision tool required for the production of plastic parts. Its main purpose is to replicate the desired geometry of the final plastic part by transforming molten plastic into its final shape and dimensional details. Currently, the design of an injection mold is a highly interactive and manual process involving substantial knowledge of multiple areas, such as mold design features, mold making processes, molding equipment and part design, all of which are highly coupled to each other. The main challenge is to design and produce a mold that is straightforward to manufacture, while providing uniform filling and cooling of plastic parts. At the same time the tool has to be strong enough to withstand millions of cyclic internal loads from injection pressures and external clamp pressures, in order to assure the target part's reproducibility (Beaumont

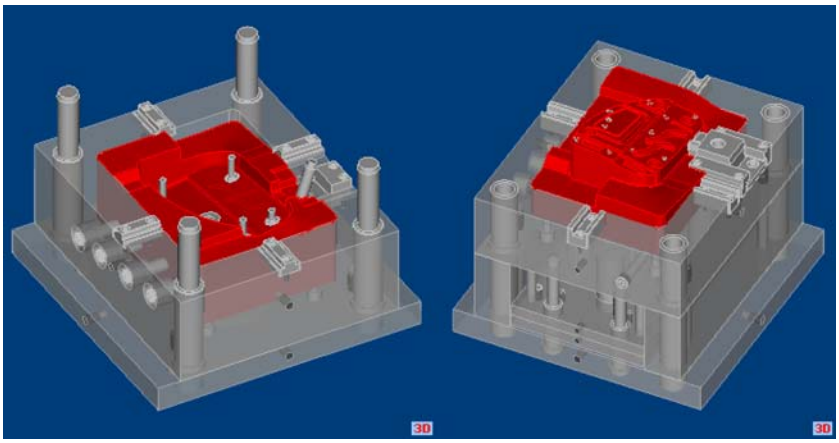

Fig. 1 Typical halves of an injection mold: cavity (*left*) and core (*right*) (Centimfe 2000)

et al. 2002). In this sense, an injection mold can be seen as a mechanical structure with some functional subsystems, such as the feeding system, heat-transfer system, structural system and ejection system. Usually, this structure is composed of two halves, where the top half of the mold is commonly referred to as the cavity half or the fixed half of the mold. The bottom half is known as the core or movable half (Fig. 1). In some cases, the cavity and core halves can be switched.

It is common for the cavity to be machined directly in the cavity inserts (dark elements), but sometimes it includes an injection clamping and a cavity retainer plate (Fig. 2). In less demanding cases, the cavity is machined directly into a cavity plate, which avoids the use of the retainer plate. The path for the melt (liquid plastic) to travel from the injection machine to the parting line is defined by a sprue brushing, which may feed directly a cavity (at a single gate point), or a runner in a multi-cavity (more than one part injected for each injection cycle) or a multi-gates point part (more than one gate point per part). During mold opening—for cold runner systems—the plastic sprue and runners are pulled from the sprue bushing by the ejection system, while for hot runner systems, the runners stay molten and are ejected during the molding cycle.

Typically, the other half of the mold contains the core and the ejection system. The core usually refers to the portion of the two mold halves where there are protrusions, onto which the forming plastic part will shrink and to which it will adhere during mold opening. The part is then usually pushed off the core by a mechanical ejection system. In order to release the part after cooling, some space is normally provided to allow movement (ejector stroke) of the ejector plates to which ejector pins are attached. This back and forth movement is assured by a hydraulic cylinder to

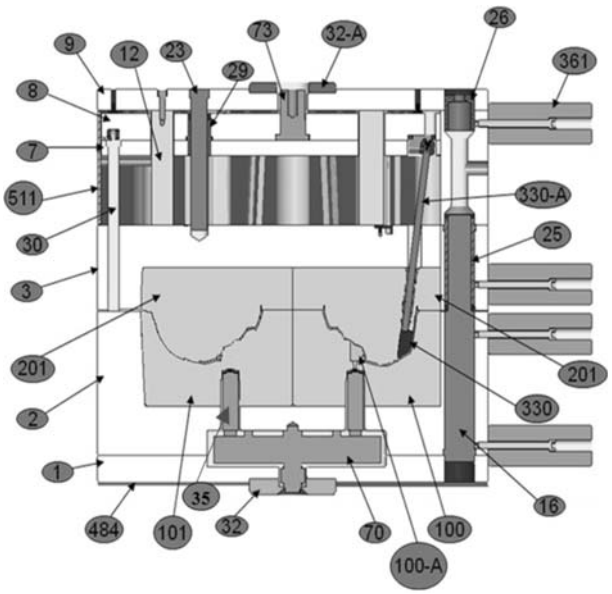

Item	Designation	Item	Designation
1	Injection clamping plate	32-A	Locating ring
2	Cavity retainer plate	35	Sprue bushing
3	Core retainer plate	70	Mainfold
7	Ejector pin plate	73	K.O.
8	Ejector pin retainer plate	100	Cavity insert
9	Ejection clamping plate	100-A	Sub-insert
12	Support pillar	101	Cavity insert
16	Leader pin	201	Core insert
23	Ejector plate pin	330	Jinggle pin
25	Guide bushing	330-A	Jinggle pin rod
26	Centering sleeve	361	Mold floor support
29	Ejector plate bushing	484	Insulator plate
30	Return pin	511	Ejector protection plate
32	Locating ring		

Fig. 2 Cross-sectional view of a common mold assembly (Vasco et al. 2007 with authors' permission)

which the ejector plate is attached. Based on this cycle, the main components of a typical injection mold, and respective functions, are as follows:

(a) Feeding System (including the venting system). Its main function is to channel the molten plastic material coming from the injection nozzle of the molding machine and distribute it into each cavity, through the runners and respective gate points. Generally, injection molds can be classified as either "cold runner" or "hot runner" molds. A cold runner refers to a mold in which the feeding system is cooled, solidified and ejected with the molded part in each molding cycle. In the case of a hot runner mold, the runner is kept in a molten state, avoiding a runner that must be refilled and discarded in each cycle. The hot runner system is typically composed of two components: the manifold and the drop(s). The venting subsystem must allow for gas release, because when the melt enters into the cavity the displaced air must have a means to escape. The design of this subsystem depends on the part's geometry, its position in the mold and its gating;
(b) Heat-transfer System. It supplies the mold with a system of cooling channels, through which a coolant is pumped. Usually, its main function is to remove heat from the mold, so that—once filled—the part is sufficiently rigid to be demolded. Note that given the fast cycle time of most machines that the coolant flow is continuous and thus some amount of heat evacuation is always ongoing;
(c) Ejection System. Its main function is to knock out the injection molded parts, in order to release them from the mold. Typically, after the mold is opened, the hydraulic cylinder of the injection machine will actuate the ejection system to move forward, pushing the molded parts out. It is critical that the ejection system does not cause damage (marks) to completed parts;
(d) Structural System. It must allow the mold (tool) to be coupled into the injection machine and assure the overall assembly of its components. It is also necessary to guarantee the alignment and guiding of the mold. According to the type of mold, it involves several metal plates to form a rigid body where some components are assembled together (e.g. locating ring; guide pins and guide bushings, amongst others);
(e) Others: for complex plastic parts, some other mechanisms, such as slides, lifters, unscrewing devices, amongst others, might also be necessary.

Therefore, the mold design optimization must encompass the optimization of four main highly-coupled systems, namely the Structural, Feeding, Heat-Exchange and Ejection systems, where each one is characterized by one or more local objective functions, in order to assure satisfaction of both final part and manufacturing process requirements. Globally, the mold as a system involves the optimization of two main functions, namely the mold's cost and performance (Table 1). At this stage, the mold's performance will be evaluated by its *cycle time*. The *cycle time* is defined as the time required from initial injection of a part, through cooling and ejection to the point where the next part is ready to be injected. It is the major attribute of injection molding productivity. Part tolerances and uniformity are set as constraints.

Table 1 Subsystems and objective functions for injection mold design

System	Global objectives
Injection mold	Min cycle time
	Min cost
Subsystem	Local objectives
Feeding	Min volume
	Min pressure drop
Heat-exchange	Max heat transfer
Ejection	Min marks
Structural	Min bending
	Min deflection

2 Related research

The design of an injection mold is considered critically important to product quality and efficient processing, as well as a determining factor for the economics of the entire process (Chan et al. 2003; Low 2003). In this sense, and in order to achieve high levels of product quality in less time, both academia and industry have been looking for new methods to address mold design. Therefore, a lot of scientific research has been done on mold design and its related fields over the last years, mostly on Knowledge-Based (KB) methods (this approach is justified by the extensive empirical knowledge about mold component functions). Examples of work in this area are IKB-MOULD (Mok et al. 2001), a 3D CAD KB (Chan et al. 2003) and ESMOLD (Chin and Wong 1996). According to Chan et al. (2003), one emergent area of research in the injection molding field attempts to generate automatically the design of mold tool components. Although, due to high complexity and significant mold component interactions, some authors (Chan et al. 2003; Low 2003) consider this approach not to be feasible for the automatic generation of an entire injection mold. Thus, this new approach has been used only to solve particular aspects of mold design. As examples of this

research thrust, Mehnen et al. (2004) studied the automation of Heat-Exchange subsystem design while Lam et al. (2004b) pursued a multi-objective approach with integration of Genetic Algorithms and CAE. On the subject of optimal feeding subsystems, Lee and Lin (2006) used FEM, Taguchi's method and an abductive network to select the best parameters. Lam et al. (2004a) proposed an automated gate optimization routine and Shen et al. (2004) developed a modified hill-climbing algorithm in order to determine the best gate location. These examples highlight the fact that research in injection mold design optimization is underway, but generally involves only one particular aspect of the total design. In our opinion the inexistence of a mold's subsystem integration (which points out the coupled relations) and the inadequate exploration of the feasible design space are limitations that must be overcome. In this sense, it is important to optimize the mold as a system through integration of its main subsystems.

3 Proposed approach

Currently, due to market pressure to reduce the time-to-market of products, the lead-time available for designing and making injection molds is decreasing. Rather than taking several months, mold design must now be accomplished in a matter of 2–4 weeks, depending on part complexity. Additionally, during the mold design process, customers oftentimes impose several changes to the plastic part geometry and other attributes, requiring fast modifications of the mold. Therefore, molds makers are compelled to shorten both lead times and cost, as well to accomplish higher levels of mold performance. This will only be possible with new design approaches. For all the reasons previously mentioned, a framework based on MDO, that aims to optimize the mold design as a system, was developed. The main design loop of the developed framework, where process integration is made by blocks representing its individual modules (Fig. 3), starts with a geometrical configuration of the initial mold solution, designed according to best practice guidelines. Then, the Geometry handler module calculates the geometrical and physical dimensions that will be used in the following steps and creates the Parasolid file needed by the subsequent analysis. Phenomena analyses are, at this stage, carried out by some analysis codes that use simplified mathematical models to characterize the main injection molding modules: the Structural, the

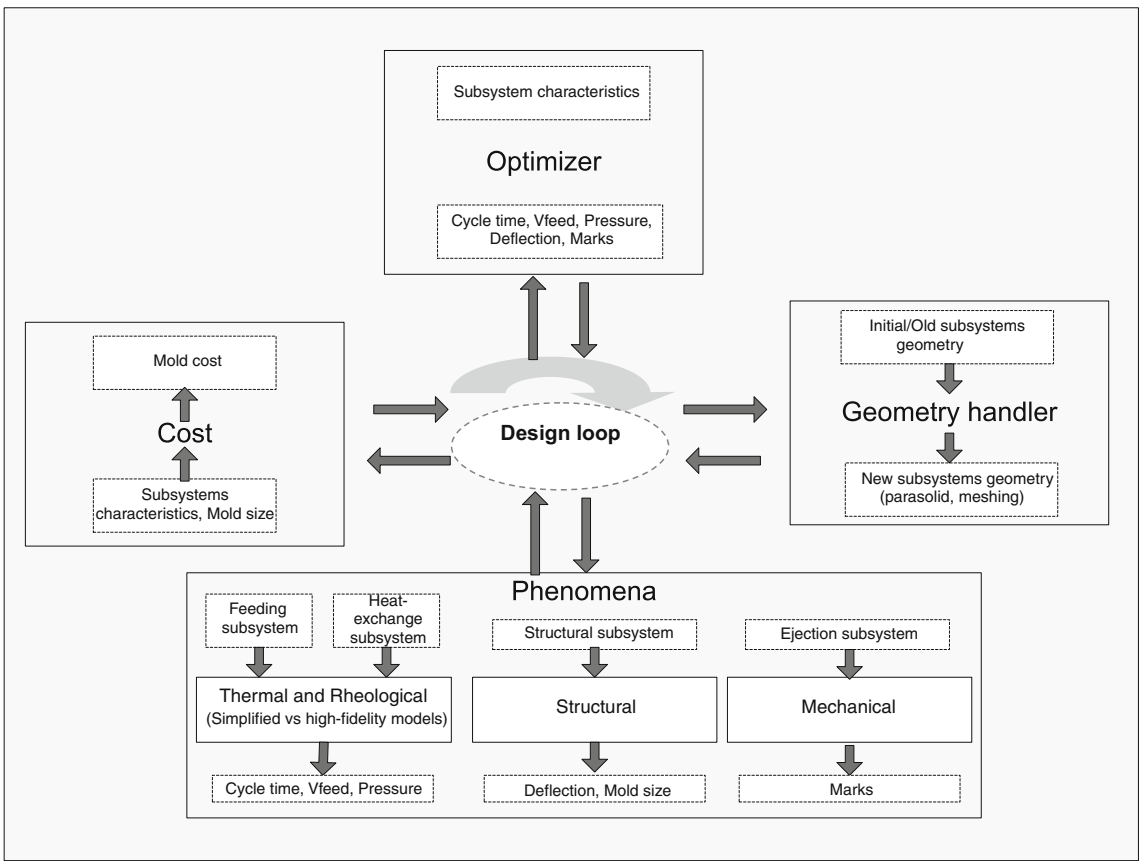

Fig. 3 Framework process integration

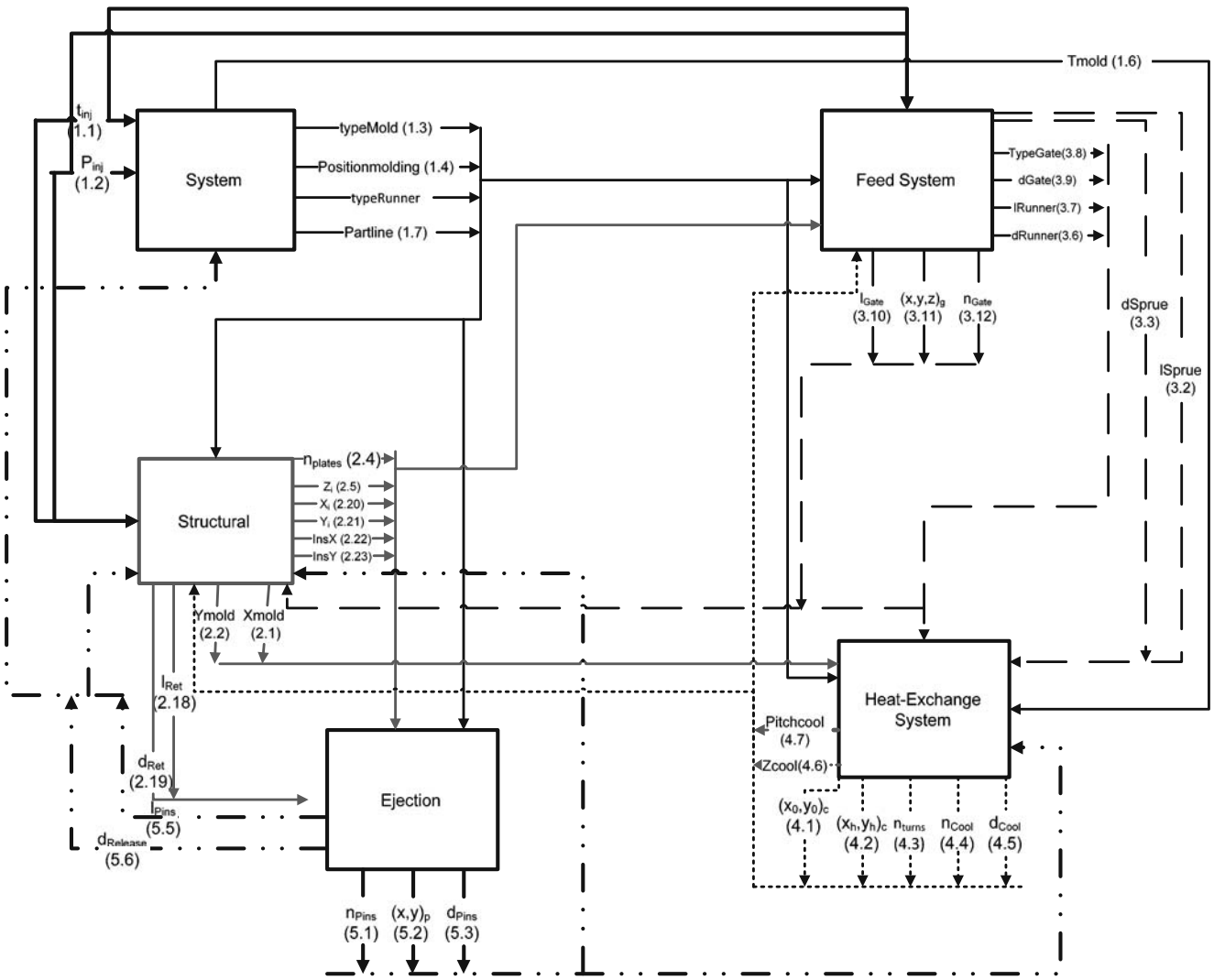

Symbol		Designation	Symbol		Designation	Symbol		Designation
1.1	t_{inj}	Time of injection	**2.20**	X_i	Final distance on X coordinate for plate i	**4.1**	$(x_0,y_0)_c$	Initial Coordinates line i
1.2	P_{inj}	Injection pressure	**2.21**	Y_i	Final distance on Y coordinate for plate i	**4.2**	$(x_h,y_h)_c$	Final Coordinates line i
1.3	typeMold	Type of mold	**2.22**	InsX	Distance on X coordinate of cavity insert	**4.3**	n_{turns}	Number of changes in position of cooling channel
1.4	Positionmolding	Position of molding on the partition plane	**2.23**	InsY	Distance on Y coordinate of cavity insert	**4.4**	n_{cool}	Number of cooling channels
1.5	typeRunner	Type of runner	**3.2**	l_{Sprue}	Length of sprue	**4.5**	d_{cool}	Diameter of cooling channel
1.6	Tmold	Temperature of mold	**3.3**	d_{Sprue}	Diameter of sprue	**4.6**	Zcool	Distance on Z from cavity surface to the center of cooling line
1.7	Partline	Parting line	**3.6**	d_{Runner}	Diameter of runner	**4.7**	Pitchcool	Pitch betwen cooling channels
2.1	Xmold	Distance of mold on X coordinate	**3.7**	l_{Runner}	Length of runner	**5.1**	n_{Pins}	Number of ejection elements
2.2	Ymold	Distance mold on Y coordinate	**3.8**	typeGate	Type of gate	**5.2**	$(x,y)_p$	Position of ejection element p
2.4	n_{plates}	Number of plates	**3.9**	d_{Gate}	Diameter of gate	**5.3**	d_{Pins}	Diameter of ejection element
2.5	Z_i	Final distance on Zcoordinate for plate i	**3.10**	l_{Gate}	Length gate	**5.5**	l_{Pins}	Length of ejection element
2.18	l_{Ret}	Lenght of return elements	**3.11**	$(x,y,z)_g$	Position of each gate	**5.6**	$d_{Release}$	Distance of part's release
2.19	d_{Ret}	Diameter of return elements	**3.12**	n_{Gates}	Number of gates			

Fig. 4 Block diagram for injection mold modules

Feeding, the Ejection and the Heat-Exchange subsystems. Later, as future research, these phenomena will be model by more accurate and realistic approximations through the integration of high-fidelity numerical models (e.g. Moldflow code—www.moldflow.com).

The system level of this framework involves the initial design decisions, such as type of mold, type of feeding system, etc. and the integration of the functional modules as interlinked subsystems. The respective inputs and outputs of each module were determined (Fig. 4), and a block diagram was built in order to identify the feedforward and feedback paths between the different modules. It is important to note that the mapping is generic and was established independently of specific plastic part and injection machine characteristics (i.e. these modules and their relations are present in every mold design problem). This approach allows the mathematical formulation of the mold design as a multidisciplinary system design problem. The multidisciplinary processes considered were *rheological,* which seeks to model and evaluate the mold filling process, *thermal,* encompassing heat transfer, *mechanical*, concerning the mold's physical movements, and, finally, *structural* (mainly represented by the number of plates and dimensions of each plate) aiming to minimize the mold's deformation induced by compressive and bending stresses. Some assumptions have been made to simplify this MDO approach to injection mold design. For example, issues like the spatial collisions between some of the mold's elements (e.g. pins, cooling lines, fixing elements, venting, amongst others), as well as the design of more complex elements, like slides and lifters, have not been taken into account. Also, a reliable cost model (both for design and tool cost, as well as part manufacturing cost) has not yet been developed. For this reason, at the present stage the mold design will be optimized for minimum *cycle time*. In order to undertake a first multi-objective optimization, the *cycle time*, as well two local objectives, namely, the *volume of feeding system* and the *injection pressure drop*, will be used as indicators of the mold's performance.

The *cycle time* is computed considering that the injection molding process has five main stages (Rosato et al. 2001). The first one, designated as *Plasticizing (1)*, involves the heating and melting of the plastic in the plasticator. The second stage, *Injection (2)*, encompasses a shot of melt into the closed mold. The third stage, named *Afterfilling* or *Packing (3)*, aims to prevent back flow and compensates for the decrease in volume of melt during solidification. The fourth, the *Cooling* stage *(4)*, involves the molded part cooling in the mold until it is sufficiently rigid to be ejected. Finally, the last stage, *Release (5)*, allows removal of the part by hydraulically opening and closing the mold to start the next cycle (Fig. 5).

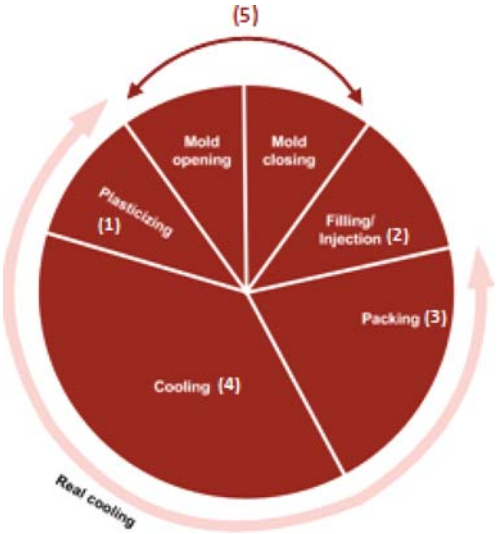

Fig. 5 Main stages of injection molding

Based on this assumption, the cycle time is calculated as the sum of each of the stage times. However, plasticizing time *(1)* was not considered in cycle time computation, since it occurs simultaneously with the cooling and packing stages of the previous part. Regarding filling time *(2)*, which depends mostly on process conditions, it was assumed as a reasonable imposed (user selected) value, similarly to the modeling procedure in Moldflow. This is a realistic assumption and allows comparison of solutions modeled by the proposed framework and verified by Moldflow.

The cooling stage, which in fact begins with mold filling and finishes when enough heat has been removed from the part in order to eject it without distortion, is the most important stage, since it absorbs about 80% of the cycle time (Qiao 2006). The heat exchange between plastic and coolant, which occurs at this stage through thermal conduction, can be described by Fourier's differential equation (Menges et al. 2001). Since heat is mainly removed in one direction (thickness direction), heat-transfer is usually described using a one dimensional description (Menges et al. 2001; Kazmer 2007). Following this approach, Fourier's differential equation can be reduced to:

$$\frac{\partial T}{\partial t} = \alpha \frac{\partial^2 T}{\partial z^2} \tag{1}$$

where α is the thermal diffusitivity, T is the temperature, t is time and z is the thickness direction coordinate. Assuming that immediately after injection the melt temperature in the cavity has a uniform constant value of T_{melt}, and that the temperature of the cavity walls jumps abruptly to the constant value T_{cool}, which remains constant, the cooling

time *(4)* for a strip plane geometry can be estimated using the previous equation, leading to the following expression (Kazmer 2007):

$$t_{cool} = \frac{s^2}{\pi^2 \alpha} \ln\left(\frac{8}{\pi^2}\frac{(T_{melt} - T_{cool})}{(T_{demol} - T_{cool})}\right) \tag{2}$$

where s is the wall thickness assuming the plastic part as a strip plate, T_{melt} is the melting temperature, T_{cool} is the cavity wall temperature and T_{demol} is the mean demolding temperature (the temperature at which the material is rigid enough to be ejected). Assuming that the time required for cooling the feeding system is longer than the time needed to cool the part itself (this is a necessary constraint to avoid premature freezing inside the part which could lead to incomplete filling), the bottleneck of the cooling process will be the feeding system, or more precisely the *Sprue* (biggest component of this subsystem, since it must supply the entire feeding system with enough melt). Due to the conical shape of this component (Menges et al. 2001), the previous generic equation (1) must be replaced by:

$$t_{cool} = \frac{\overline{d}^2_{Sprue}}{23.1\alpha} \ln\left(0.692\frac{(T_{melt} - T_{cool})}{(T_{demol} - T_{cool})}\right) \tag{3}$$

where $\overline{d}_{Sprue}$ is the sprue mean diameter. Note that both (2) and (3) are solutions of (1), but (2) is valid for strip plates, while (3) assumes a cylindrical geometry.

The post-filling time *(3)*, generally known as *packing time*, is determined based on the gate dimensions (Kazmer 2007). The packing stage has as its main function to force additional melt into the cavity, after the filling stage, in order to compensate for volumetric shrinkage of the part and to avoid any back flow of melt. Therefore, if the gate is too small the melt will prematurely solidify and no additional material will enter into the cavity (packing does not occur). If it is too large, the gate will take more time than necessary to solidify, which results in a longer pack time. Thus, the packing stage time must end with the gate freeze-off. The necessary cooling time for gates (i.e. gate freeze-off) is determined using an expression according to (4):

$$t_{pack} = \frac{d^2_{Gate}}{23.1\alpha} \ln\left(0.692\frac{(T_{melt} - T_{cool})}{(T_{demol} - T_{cool})}\right) \tag{4}$$

where d_{Gate} is the gate diameter.

The mold opening time is calculated as the ratio of the mold opening distance (designated as $d_{Release}$) and the mold opening velocity. The velocity of mold opening (v_{open}) was based on Kazmer's regression (Kazmer 2007: page 129), which states that the velocity is a logarithmic function of the ratio between the clamping force (i.e. the force needed to hold the mold closed expressed in tons) and a reference force of 1 ton (5).

$$v_{open}\,[\text{mm/s}] = 184 + 13\log\left(\frac{F_{clamp}}{F_{ref}}\right) \tag{5}$$

Where v_{open} is expresses in millimeters per second. Since the clamping force can be computed as the injection pressure (P_{inj}) times the projected area of molding (A_{proj}), the mold opening time can be calculated using (6).

$$t_{open} = \frac{d_{Release} 1 \times 10^3}{184 + 13\log\left(\frac{P_{inj} A_{proj} 1\times 10^{-3}}{9.8 F_{ref}}\right)} \tag{6}$$

In this work, it is assumed that the time to open is equal to the time to close the mold (i.e. the time to release the part *(5)* is equal to two times the opening time). In summary, the theoretical cycle time (objective function), which involves the summation of cooling time (expressed by the necessary time to cool the Sprue) plus the packing time (which is limited by gate's freezing), and, finally, the time to open and to close the mold, that can be described by the following expression:

$$\begin{aligned} Cycle\ time = {} & \frac{\left[d_{Sprue} + \tan\left(\frac{\alpha_{Sprue}\pi}{180}\right) l_{Sprue}\right]^2}{23.1\alpha} \\ & \times \ln\left(0.692\frac{(T_{melt} - T_{cool})}{(T_{demol} - T_{cool})}\right) \\ & + \frac{d^2_{gate}}{23.1\alpha} \ln\left(0.692\frac{(T_{melt} - T_{cool})}{(T_{demol} - T_{cool})}\right) \\ & + 2 \times \frac{d_{Release} 1 \times 10^3}{184 + 13\log\left(\frac{P_{inj} A_{proj} 1\times 10^{-3}}{9.8 F_{ref}}\right)} \end{aligned} \tag{7}$$

Considering Fig. 5 the plasticizing time *(1)* is neglected since it occurs in parallel with the other processes for the preceding part. Also, the injection time *(2)* is very small compared to the other times in (7) and is assumed as a constant value (it was assumed 1.5 s for filing time). Finally, the cooling time *(4)* is not the total time doing which cooling occurs, but only the excess cooling time required for the Sprue to freeze (Fig. 6).

Note that $\overline{d}_{Sprue}$ can be determined based on the geometrical characteristics of the Sprue as:

$$\overline{d}_{Sprue} = d_{Sprue} + \tan\left(\frac{\alpha_{Sprue}\pi}{180}\right) l_{Sprue} \tag{8}$$

where d_{Sprue} is the initial diameter, l_{Sprue} is the length and α_{Sprue} is the draft angle.

To optimize cycle time, the following constraints are considered:

$$-P_{inj}+\frac{32\left(l_{Sprue}+l_{Runner}+l_{Gates}+l_{part}\right)\varphi\bar{v}_F\eta_{aeff}}{\left(\frac{2MaxYM_{\text{int}}}{MaxY+M_{\text{int}}}\right)^2}\leq 0 \tag{9}$$

The pressure demand to counter the resistance to flow in plate (flow length/wall thickness ratio derived from Hagen–Pouseuille's law (Menges et al. 2001)).

$$P_{inj}-\frac{F_{clamp\,\max}}{A_{proj}}\leq 0 \tag{10}$$

The melt pressure acting in the projected area of mold cavities must not surpass the maximum clamp force (required to hold the mold closed during operation).

$$l_{Sprue}-Z_{cav}-Z_{plate\_1}=0 \tag{11}$$

To assure geometric feasibility, the length of Sprue must be equal to plate's distance starting in injection nozzle until partition plane.

$$-d_{Gate}+2\left[\frac{(3+1/n)\,\dot{V}}{\pi\dot{\gamma}_{\max}}\right]^{1/3}\leq 0 \tag{12}$$

Shear rate for flow in gates must not surpass the maximum allowable shear (Power law is assumed, which is a conservative approach).

$$-d_{Release}+MaxOpen-Z_{mold}\leq 0 \tag{13}$$

Distance of part's release must not surpass the maximum free open distance of mold.

$$-d_{Release}+2.5MaxZ\leq 0 \tag{14}$$

The distance of mold opening must assure part's release.

$$-d_{Sprue}+d_{Runner}\sqrt{n_{downstream}}\leq 0 \tag{15}$$

Sprue must have enough capacity to fulfill all the downstream runners.

where l_{Runner} is the runner length, l_{Gates} is the gates length and l_{part} is the part length, φ represents a constant ratio between width and thickness (which is equal to 1.5, when width is much bigger than thickness), $\bar{v}_F$ is the velocity of the flow front and η_{aeff} is the apparent effective viscosity; *MaxY* and *MaxZ* are the part maximum distances along the Y and Z directions, respectively; $F_{clampmax}$ is the maximum clamping force; Z_{cav}, Z_{plate_1} and Z_{mold} correspond to the distance in the Z direction for the cavity plate, plate one and for the complete mold, respectively; n is the power index of the Power Law model, $\dot{V}$ is the volumetric flow rate and $\dot{\gamma}_{\max}$ is the maximum shear rate for the plastic; *MaxOpen* is the maximum distance in Z direction for the mold. The runner diameter is defined by d_{Runner} and, finally, $n_{downstream}$ is the number of streams of each ramification. The design variable bounds are defined as follows:

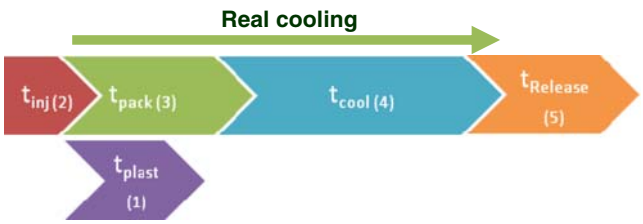

Fig. 6 Timeline of each injection molding stage

Lower and upper bounds:

$$d_{Sprue}\leq 0.02 \tag{16}$$

$$1\leq\alpha_{Sprue}\leq 4 \tag{17}$$

$$0.0005 \leq d_{Gate} \leq 0.003 \tag{18}$$

$$0.0005 \leq l_{Gate} \leq 0.001 \tag{19}$$

Additional Constraints (for single objective optimization):

$$\text{Volume of feeding system} \quad <= \quad 0.3 Vpart \tag{20}$$

$$\text{Pressure drop} \quad <= \quad 0.5 P_{inj} \tag{21}$$

where V_{part} is the total volume of the molded plastic part. The minimization of wasted material is defined based on the volume of the feeding system (cold runner system), computed by:

$$V_{feed} = \frac{\pi}{4}\left(\bar{d}^2_{Sprue} l_{Sprue} + n_{downstream} n_{Ramif} d^2_{Runner} l_{Runner} + d^2_{Gate} l_{Gates} n_{Gates}\right) \tag{22}$$

where n_{Ramif} and n_{Gates} are the number of ramifications of the runner and number of gates per each plastic part, respectively.

The minimization of pressure drop is determined using the equation of motion, where the force due to pressure drop along the flow (caused by the viscous flow in the channel) must be equal to the force resulting from shear stresses. Both occur along the length of the melt flow. Therefore, using the Power Law Model, which has been shown to provide accurate results, that states that viscosity is an exponential function of the shear rate, it is possible to estimate pressure drop as a function of the volumetric flow rate. For a channel with a circular shape, the pressure drop estimate is given by:

$$\Delta P = \frac{4kL}{D}\left[\frac{\left(3+\frac{1}{n}\right)\dot{V}}{\pi\left(\frac{D}{2}\right)^3}\right]^n \tag{23}$$

where k is the viscosity evaluated at a shear rate of one reciprocal second, n is the power law index, $\dot{V}$ is the volumetric flow rate, D is diameter and L is the channel length. Based on this expression, the total pressure drop caused by the feeding system is established as:

$$\Delta P = \frac{4kl_{Sprue}}{\bar{d}_{Sprue}}\left(\frac{\left(3+\frac{1}{n}\right)\dot{V}}{\pi\left(\frac{\bar{d}_{Sprue}}{2}\right)^3}\right)^n + \frac{4kl_{Runner}}{d_{Runner}}\left(\frac{\left(3+\frac{1}{n}\right)\dot{V}}{\pi\left(\frac{d_{Runner}}{2}\right)^3}\right)^n + \frac{4kl_{Gates}}{d_{Gates}}\left(\frac{\left(3+\frac{1}{n}\right)\dot{V}}{\pi\left(\frac{d_{Gates}}{2}\right)^3}\right)^n \tag{24}$$

The mathematical problem for the design of an injection mold is therefore defined.

However, since the mold design is highly dependent on the plastic part geometry, it was necessary to establish a specific plastic part to apply the MDO framework. The benchmark plastic part studied (ABS Cycolac MG47 produced by GE Plastics—USA) is illustrated in Fig. 7. The simple geometry of the plastic part was adopted, because at this stage of research, the developed framework does not include the design of complex elements, such as sliders or lifters, which are necessary to guarantee undercuts of the plastic part (for this particular case, these elements are not required). Regarding material selection, ABS Cycolac MG47 was adopted since it is a well characterized material, for which all necessary information is included in most material industry databases.

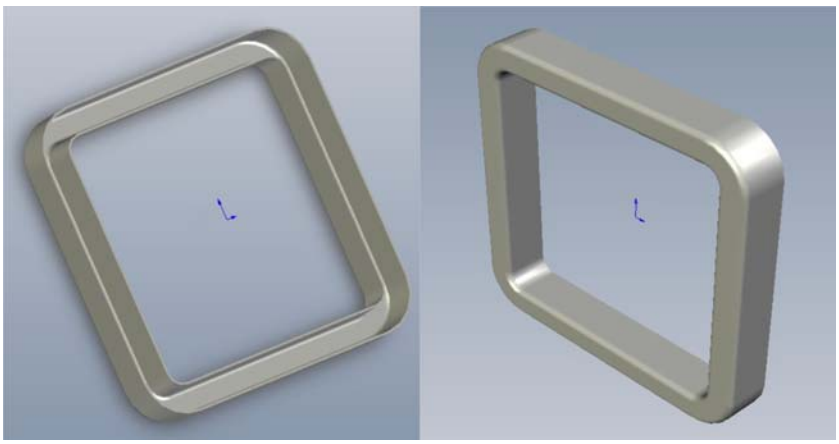

Fig. 7 The designed benchmark part back views

4 Single objective optimization

In a first optimization procedure, one single objective function was considered, namely cycle time minimization. The remaining objective functions, concerning the Structural, Feeding, Heat-Exchange and Ejection subsystems, were included in the model as constraints. Cost minimization is not yet included in the model, since this variable is mostly a function of part's size and complexity, which at this stage were considered as fixed parameters. To undertake cycle time optimization as a single objective function, a gradient-based approach was adopted. In order to select the most adequate gradient-based algorithm, some important characteristics of injection mold design were considered, namely the number and type of design variables and constraints, the feasibility of design space, the type of initial solution and the adequate simulation runtime. Based on these factors, and following iSIGHT criteria (iSIGHT-FD 2007), a brief characterization of this mold design problem was obtained (Table 2).

In this context, and considering that certain optimization techniques do not perform adequately in the presence of equality constraints (e.g., Method of Feasible Directions—CONMIN) and others are better adapted to handle problems with infeasible initial designs (e.g. penalty-based optimization techniques), some gradients based methods can be excluded. Moreover, since the mold design problem is a large-scale nonlinear programming problem (NLP) with mostly smooth non-convex nonlinear functions (there are some constraints and at least one objective that is a non smooth nonlinear function of the decision variables) the choice of optimizer can be made judiciously. Thus, the most widely used and effective methods are Generalized Reduced Gradient (GRG) and Sequential Quadratic Programming (SQP). One special advantage of the GRG method is that the extension for determining the solution of large sparse problems is conceptually simple. The availability and user-friendly nature of the GRG2 method (Lasdon et al. 1978), justified its adoption to undertake this task.

By using GRG2, the optimal solution determined corresponds to a cycle time reduction of 41.7%, as compared with the initially assumed (feasible) solution (Table 3). This initial solution was established according the practical guidelines followed by the injection molding industry, which can be observed in mold designer manuals (Centimfe 2003).

In order to assess the real improvement of the optimized designs obtained by the framework, both baseline and optimal solutions were tested using high-fidelity Moldflow code under the same processing conditions (MPI 6.1 rev 3 build 012567). Based on the data gathered (Table 4 and Fig. 8), it is possible to observe that the results produced by the proposed framework are consistent with Moldflow simulations results.

Afterwards, sensitivity analysis at the optimum point was performed. First the unnormalized sensitivity was computed evaluating the partial derivates at the optimal point. Then, these values were normalized in order to estimate the normalized sensitivity values through:

$$\frac{\Delta J/J}{\Delta x_i/x_i} \approx \frac{x_{i,*}}{J(\mathbf{x}^*)} \cdot \left.\frac{\partial J}{\partial x_i}\right|_{\mathbf{x}^*} \tag{25}$$

The computed values, which physically mean the % change in objective function per % change in design variable/parameters, can be compared in Fig. 9 for fixed parameters and Fig. 10 for design variables.

Each value indicates the percentage change in the objective function per percentage of change in the respective design variable or parameter. Based on these values, one can verify that the most sensitive variables are the sprue diameter dSprue (d_{Sprue}) and the sprue cone angle DraftSprue (α_{Sprue}). This result is physically consistent, since the cycle time is primarily determined by mold temperature control, i.e. cooling time (Rosato et al. 2001). Therefore, because

Table 2 Main characteristics of mold design mathematical problem formulation

Factors	
Number of design variables	High (>20)
Number of constraints	Low (<1,000)
Type of design variables	Real; integer and categorical
Objective/constraints functions	Non linear
Constraints type	Inequality/equality
Feasible space	Non-convex and discontinuous
Initial point	Feasible
Simulation run time	Short (see Table 7)

Table 3 Optimal design solution obtained by the GRG2 algorithm

Design variables		Initial point	Optimal
P_{inj}	Pa	1.80E+08	2.11E+08
$d_{Release}$	m	7.50E-02	7.50E-02
l_{Sprue}	m	9E-02	1.02E-01
d_{Sprue}	m	1.2E-03	8.49E-03
α_{Sprue}		1.0	1.0
d_{Gate}	m	0.5E-3	1.44E-03
Cycle time (s)		112.7	65.7
Ratio			−41.7%

Table 4 Comparison between results obtained by proposed framework and Moldflow numerical simulations

Design variables	Initial	Optimal
P_{inj}	1.80E+08	2.11E+08
$d_{Release}$	7.5E-02	7.50E-02
l_{Sprue}	9E-02	1.02E-01
d_{Sprue}	1.2E-02	8.49E-03
α_{Sprue}	1.0	1.0
d_{Gate}	0.5E-03	1.44E-03
	Cycle time (s)	
Framework Moldflow	112.7	65.7
	119.8	66.72

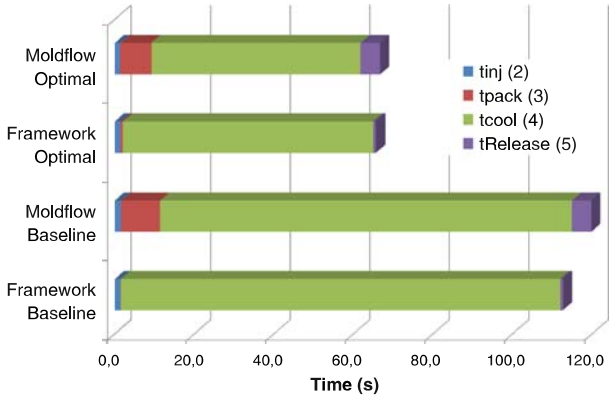

the Sprue must be large enough to feed several runners and gates, this component will be the largest of the feeding system, and requires the longest time to cool. Additionally, in order to avoid premature melt freezing in feeding channels, which can lead to incomplete filling of part(s), we imposed as constraints that the time to cool the feeding system should be longer than the time to cool the part itself. This constraint reinforces the importance of the Sprue dimensions for cycle time. Regarding the *DraftSprue*, due to its correlation with *dSprue* (Fig. 11), the previous explanations are also true for it (the higher DraftSprue, the higher the final volume of the Sprue).

Regarding the fixed parameters, the most sensitive are the thermal diffusivity and the ratio between the difference of the melt and coolant and the demolded and coolant temperatures. This is also physically consistent, since the larger the thermal diffusivity the more heat is transferred between the melt and the coolant, and consequently the faster the part's cooling. Conversely, if the difference between melt and coolant temperature increases, the quantity of heat to be removed from the part becomes higher, requiring a longer cycle time.

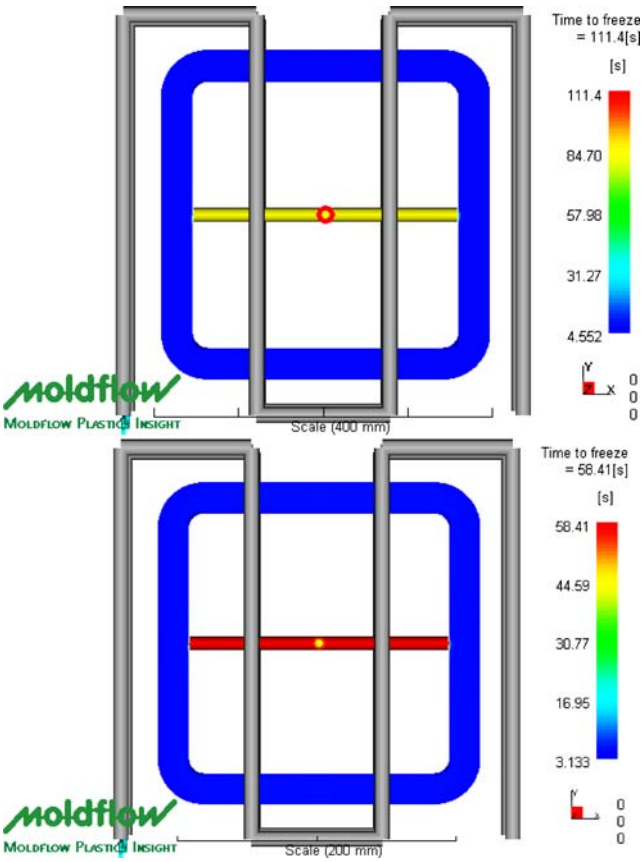

Fig. 8 Time to freeze in seconds obtained by Moldflow numerical simulations: baseline (*left*—111.4 s) and optimal (*right*—58.41 s)

5 Multiple objective optimization

In order to globally optimize the mold design as a system, both cycle time (used as a good indicator of mold technical performance) and mold cost should be used as objective functions (Table 1). However, in the absence of a reliable cost model, the multi-objective optimization performed considers one global objective, *cycle time*, and two

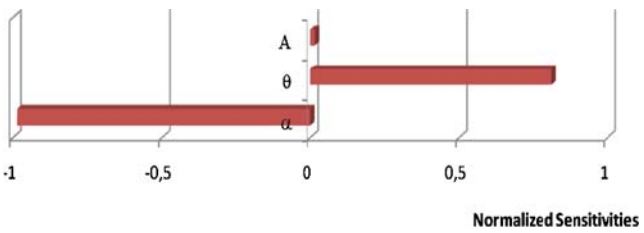

Fig. 9 Parameter normalized sensitivity values. $\theta = (T_{melt} - T_{cool})\,/\,(T_{demol} - T_{cool})$, A projected area of molded part, α thermal diffusitivity

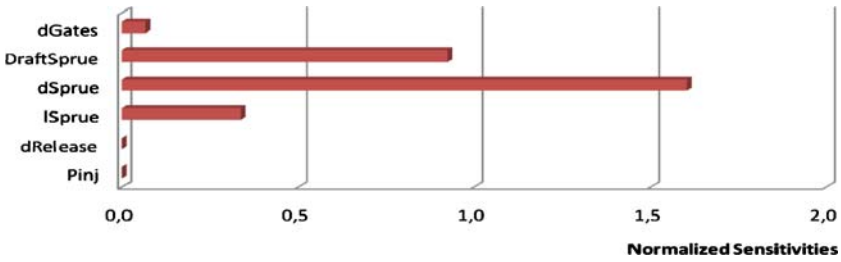

Fig. 10 Normalized sensitivity values for design variables

local objective functions, namely *injection pressure drop* and *feeding system volume* (both indicators of mold performance). The pressure drop, which is being caused by the viscous flow in the channel that generates shear stresses against the side walls, must be minimized since it reduces the injection pressure needed to inject the melt. The minimization of this variable also contributes to the mold's life time.

To undertake this optimization, a Multi-objective Genetic Algorithm (MOGA) was adopted. This is a multi-objective exploratory technique well-suited for discontinuous and non-linear design spaces. MOGA optimization was carried out using the NSGAII-Non-dominated Sorting Genetic Algorithm in iSIGHT-FD 2.5 (iSIGHT-FD 2007). The NSGA II is a non-dominated sorting based multi-objective algorithm developed by Deb et al. (2002), which alleviates the three limitations attributed to multi-objective evolutionary algorithms: computational complexity, non-elitism approach and the need for a sharing parameter. In this approach each objective is treated separately and a Pareto front is constructed by selecting feasible non-dominated designs. The NSGA-II selection process is based on two main mechanisms, "non-dominated sorting" and "crowding distance sorting". Thus, the Pareto set is constructed where each design has the best combination of objective values, so that improving one objective is impossible without sacrificing one or more of the other objectives. The tuning parameters, and respective values used for optimization are illustrated in Table 5.

An optimal design solution generated can be seen in Table 6. The Pareto points are illustrated in Fig. 12 below, whereby the original baseline solution is highlighted (highlighted point).

Even though multi-objective optimization problem does not yield a unique solution, we considered it important to have an idea of the potential improvement of the previous single-objective optimization. In this sense, the same baseline solution was compared with the previous optimal solution, where it is possible to verify that an improvement was achieved in all three objectives. This represents significant improvements for the entire injection molding process, where 2 s less (almost 2% reduction) for each cycle corresponds to 80 more parts produced per week, with approximately the same amount of material scrap and much less energy consumption (due to the 10% reduction achieved for injection pressure). Nevertheless, it is important to mention that the baseline solution was obtained following some empirical guidelines and, then, refined by a Design of Experiments study (good initial solution).

The pair-wise Pareto fronts in Fig. 12 show that there is no significant tradeoff between injection volume and cycle time. As volume increases so does cycle time. There is, however a significant tradeoff between required injection pressure and cycle time. As injection pressure is increased above 100 [MPa], cycle time can be reduced to below 100 [s]. This, however will come at the cost of tool life time and more energy consumption. There also appears to be a strong tradeoff between feeding volume and injection pressure, where for the same increase in injection pressure (100 [MPa]), the feeding volume is reduced to below 2.75E-5 [m^3].

The choice of final injection mold design should be made from the set of Pareto optimal designs, using additional

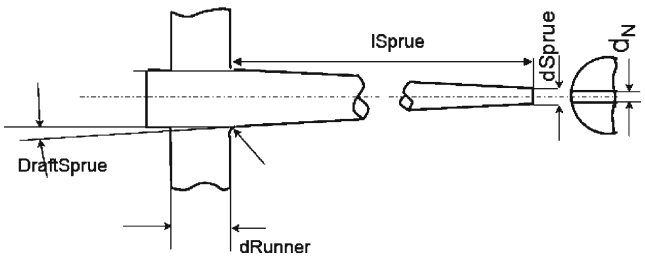

Fig. 11 Schematic design of sprue

Table 5 Tuning parameters used in NSGA-II

	Values
Population size	20
Number of generations	20
Crossover probability	0.9
Crossover distribution index	50
Mutation distribution index	100

Table 6 One Pareto solution obtained by NSGA-II

	Baseline	Optimal
d_{Gate}	0.0005	0.002
α_{Sprue}	1.0	1.0
$d_{Release}$	0.075	0.132
d_{Runner}	0.009	0.009
d_{Sprue}	0.012	0.0128
l_{Gate}	5.0E-4	5.02E-4
l_{Runner}	0.0845	0.084
$n_{downstream}$	2	2
n_{Gate}	2	2
n_{Ramif}	1	1
P_{inj}	1.8E8	1.31E8
Cycle (s)	134.18	131.84
Pressure (MPa)	98.804	89.7
V_{feed} (m^3)	2.82E-5	2.80E-5

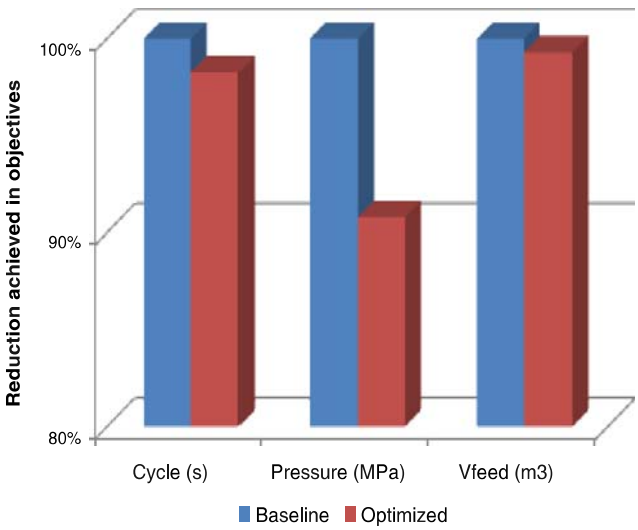

customer preferences and criteria that may not be explicitly represented in the model. For example the expected total production volume for the specific injection molded parts will be an important decision criterion to select designs along the Pareto front. The vertical bands in the parallel coordinates plot of Fig. 12 (bottom) indicate the range of feasible design variables.

It is interesting to note that runner length and diameter appear to be tightly clustered for all designs, while the number of gates, ramifications and Sprue dimensions can vary

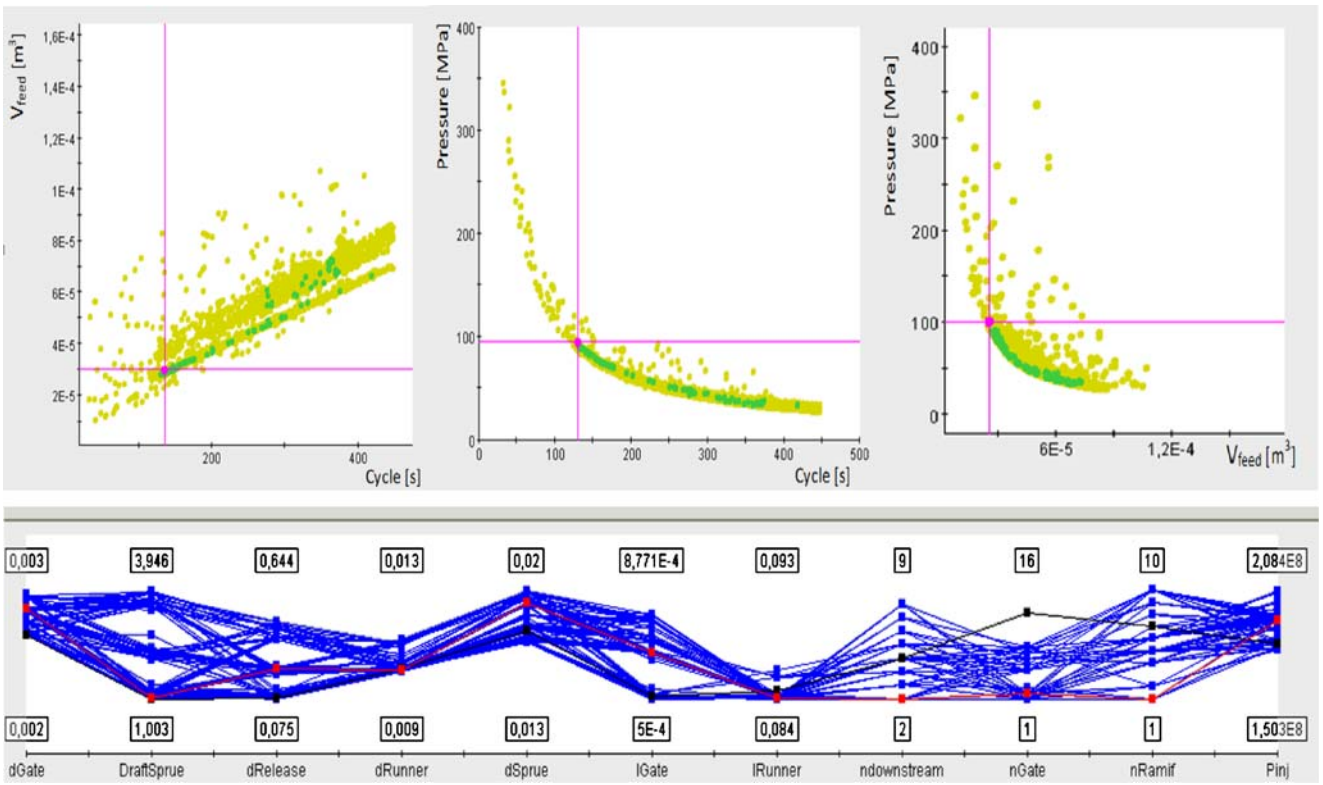

Fig. 12 Pareto solutions identified (*above*: pair-wise Pareto front, *below*: design variables parallel coordinates)

more significantly. This shows that the design details of the feeding system have a very large impact on ultimate mold performance. Among these the design of the Sprue (Fig. 12) appears to have the largest impact on overall mold performance, since productivity (because Sprue needs the longer time to cool), waste of material (because Sprue is the largest component of the feeding system) and energy consumption (because lower flow resistance of the feeding system will result in lower levels of injection pressure needed) are dependent on Sprue geometrical dimensions.

Table 7 Computational time (s)

Method	CPU computation time (s)	Functions	Evaluations	Number of feasible designs
GRG2	50	Single objective	57	41
NSGA-II	2406	Three objective	2,501	1,493
Moldflow baseline	3,416.53			
Moldflow optimal	3,764.33			

6 Conclusions and future work

The main objective of this research was to develop a framework that tackles the design of an injection molding system in a global way, through structural, thermal, rheological and mechanical domain integration. Process integration adopts a building approach by modules, where all different analysis codes are connected through an integration software (such as iSIGHT) in order to automate the iterative procedure of the optimization process. In this first attempt, which highlights how a multidisciplinary approach can help designers improve mold performance during preliminary design by selecting from the Pareto front a most suitable solution (according to experience and trade-offs amongst objectives), each module was characterized by a simplified mathematical model. It is important to note that the developed framework can be easily adapted for specific part geometries, because its modules, and respective relations, are present in every plastic injection mold. The overall framework is represented by Figs. 3 and 4.

In order to validate this framework, two optimization cases were carried out. First, using the GRG2 algorithm, our model was optimized regarding cycle time, which allowed for a 42% reduction of cycle time, when compared with a baseline solution. Secondly, multiple objective optimization was undertaken through the simultaneous minimization of cycle time, pressure drop and feeding volume. The results showed that cycle times below 100 s are possible but that they require larger injection pressures. Also, it appears that feeding system volume and cycle time are linearly correlated. This task was carried out using the iSIGHT-FD 2.5 NSGA-II heuristic based method. Both approaches point out the great potential for mold design improvement over current heuristic guidelines.

We found that gradient search with GRG2 was computationally more efficient (Table 7). However, this method could not deal, successfully, with non-smooth and discontinuous functions, whereas NSGA-II proved to be efficient, especially in highly non-linear and discontinuous design spaces. In this sense, to optimize the design of an injection molding system, the most appropriate approach will be a MOGA, like NSGA II, which performed well in multi-objective optimization. Even though, since the ultimate objective of the proposed framework is to design molds in order to reach higher levels of customer's satisfaction, one single objective function defined as a weight function of specific functional requirements was previously developed (Ferreira et al. 2007, 2008). Therefore, the computational inefficiency typically associated with GAs, and especially for MOGA that incorporates numerical simulations models, can be overcome. It is also important to mention that the mold design space is a discontinuous non-convex set. Therefore, it will be impossible to have 100% certainty that the optimal solution found is a global optimum. However, one important issue in mold's design optimization is to assure the feasibility of the design. In fact, an improved design solution is better than not finding the optimal solution, reinforcing the GA choice.

To develop a more realistic model for injection molding in the future, it will be necessary to refine the optimization model by including all important variables, especially the categorical ones (like the type of feeding system: Cold runner, Insulated runner, Insulated hot runner or Hot manifold), and expand its scope to cover the design of more complex elements, like sliders and lifters. It is also important to build and integrate in the model a reliable mold cost function. The integration of some high-fidelity models, like Moldflow, in order to get more accurate results, as well as CAD tools to be able to visualize the design solutions, is also fundamental in a fully integrated mold optimization system. In this sense, iSIGHT will be responsible for automatically running the analysis codes, accessing the outputs and changing the input data, according to the pre-defined mathematical exploration schemes. Through the integration of relevant tools, such as CAD software (e.g. Unigraphics or CATIA) as the geometry handler module, Moldflow will be responsible for thermal and rheological characterization, and Microsoft Excel and Matlab for the remaining modules (e.g. Cost, and for Structural and Mechanical modules, respectively). In order to evaluate if this approach is computationally viable, a summary of the analysis times required by the Moldflow

benchmarking, as well as the single and multi-objective optimization results presented in this paper, are illustrated in Table 7. Based on that, it is possible to observe that the computational effort of a single Moldflow simulation (>3,000 s), which represents only one evaluation, exceeds the total time required to run the entire single and multi-objective optimization procedures with simplified models, of 50 and 2,400 s, respectively. Nevertheless, since the ultimate objective of the proposed framework is to design molds in order to reach higher levels of customer satisfaction, the inclusion of high-fidelity models as Moldflow code the parametric MDO approach can be considered computationally feasible (i.e. a first estimation for its computational time is 55 h, 57 evaluations times 3,500 s for each Moldflow simulation). Finally, since the several distinct subsystems feature their own local objective functions, some of the distributed design methods, such as CO (Sobieski and Kroo 1996, 2000) and BLISS (Sobieszczanski-Sobieski et al. 1998, 2002), could also help to improve the general model. Such investigations are recommended as future work.

Acknowledgments The first author would like to express their sincere thanks to the MIT Portugal Program for their support of this research. The author is also grateful to Prof. Karen Willcox, Chris Mandy and the 16.888–ESD.77 participants for their support, and to FLAD for financial support.

References

Beaumont J, Nagel R et al (2002) Successful injection molding: process, design and simulation. Hanser, Cincinnati

Centimfe (2000) Projecto Delfim—Subprojecto Moldes

Centimfe (2003) Manual do projectista para moldes de injecção de plásticos

Chan WM, Yan L et al (2003) A 3D CAD knowledge-based assisted injection mould design system. Int J Adv Manuf Technol 22: 387–395

Chin K-S, Wong TN (1996) Knowledge-based evaluation for the conceptual design development of injection molding parts. Eng Appl Artif Intell 9(4):359–376

Deb K, Pratap A et al (2002) A fast and elitist multiobjective genetic algorithm: NSGA-II. IEEE Trans Evol Comput 6(2):182–197

Ferreira I, Cabral JA et al (2008) Customer's satisfaction evaluation of Portuguese mould makers based on the ECSI approach. In: RPD 2008—rapid product development. Oliveira de Azeméis—Portugal

Ferreira I, Cabral JS et al (2007) A new conceptual framework based on the ECSI model to support axiomatic design. In: Virtual and rapid manufacturing. Taylor & Francis, New York

iSIGHT-FD 2.5, Software package, Ver 2.5.5 (2007) Engineous software

Kazmer DO (2007) Injection mold design engineering. Hanser, Cincinnati

Lam YC, Britton GA et al (2004a) Optimisation of gate location with design constraints. Int J Adv Manuf Technol 24:560–566

Lam YC, Zhai LY et al (2004b) An evolutionary approach for cooling system optimization in plastic injection molding. Int J Prod Res 42(10):2047–2061

Lasdon LS, Warren AD et al (1978) Design and testing of a generalized reduced gradient code for nonlinear programming. ACM Trans Math Softw 4:34–50

Lee KS, Lin JC (2006) Design of the runner and gating system parameters for a multi-cavity injection mould using FEM and neural network. Int J Adv Manuf Technol 27:1089–1096

Low MLH (2003) Application of standardization for initial design of plastic injection moulds. Int J Prod Res 41(10):2301–2324

Mehnen J, Micheltisch T et al (2004) Evolutionary optimization of mould temperature control strategies: encoding and solving the multiobjective problem with standard evolution strategy and kit for evolution algorithms. Proc Inst Mech Eng 218(Part B): 657–665

Menges G, Walter M et al (2001) How to make injection molds. Hanser, Cincinnati

Mok CK, Chin KS et al (2001) An interactive knowledge-based CAD system for mould design in injection moulding processes. Int J Adv Manuf Technol 17:27–38

Qiao H (2006) A systematic computer-aided approach to cooling system optimal design in plastic injection molding. Int J Mech Sci 48:430–439

Rosato DV, Rosato DV et al (2001) Injection molding handbook. Kluwer, Dordrecht

Shen C-Y, Yu X-R et al (2004) Gate location optimization in injection molding by using modified hill-climbing algorithm. Polym-Plast Technol Eng 43(3):649–659

Sobieski I, Kroo I (1996) Aircraft design using collaborative optimization. In: AIAA 34th aerospace sciences meeting and exhibit. Reno, NV

Sobieski IP, Kroo IM (2000) Collaborative optimization using response surface estimation. AIAA J 38(10):1931–1938

Sobieszczanski-Sobieski J, Agte JS et al (1998) Bi-Level Integrated System Synthesis (BLISS). N. A. a. S. Administration. Hampton, Virginia

Sobieszczanski-Sobieski J, Altus TD et al (2002) Bi-Level Integrated System Synthesis (BLISS) for concurrent and distributed processing. In: 9th AIAA/ISSMO symposium on multidisciplinary analysis and optimization. Atlanta, Georgia, pp 1–11

Vasco J, Capela C et al (2007) Material selection for high performance moulds. In: Improving quality & tool efficiency within injection moulding—SPE meeting, K2007. Dusseldorf Society of Plastic Engineers